scientific data

Check for updates

OPEN

DATA DESCRIPTOR

A Transcriptomic Dataset of Embryonic Murine Telencephalon of *Fmr1*-Deficient Mice

Sara Ebrahimiazar[1], Takako Kikkawa[1]✉, Yohei Minakuchi[2], Satoshi Miyashita[3], Shyu Manabe[1], Mikio Hoshino[3], Atsushi Toyoda[2] & Noriko Osumi[1]✉

Fragile X syndrome (FXS) is a neurodevelopmental disorder caused by mutations in the *fragile X messenger ribonucleoprotein 1* (*FMR1*) gene. FXS patients exhibit autistic behaviors and abnormal brain structures, with notable sex differences. However, the mechanisms by which *Fmr1* deficiency leads to these sex differences during brain development remain unclear. In this study, we performed bulk RNA sequencing on telencephalon samples of *Fmr1*-knockout mice of both sexes at embryonic day (E) 14.5, i.e., at the peak of neurogenesis. Clustering analysis revealed gene expression differences influenced by *Fmr1* gene dosage and sex. We found that majority of the transcripts were shared between male and female sample groups, while a smaller number were unique to each sex. Our dataset underscores the importance of studying brain development during the embryonic period to detect sex-dependent genetic factors which contribute to neurodevelopmental disorders.

Background & Summary

Neurodevelopmental disorders (NDDs) encompass a range of brain development abnormalities that lead to cognitive impairments and behavioral deficits. Fragile X syndrome (FXS) is a well-known NDD, associated with a broad spectrum of behavioral symptoms, including autism, intellectual disability, anxiety, and hyperactivity[1]. The prevalence of FXS is estimated at 1.4 per 10,000 males and 0.9 per 10,000 females[2]. Comparisons between male and female children with FXS have revealed larger volumes of the total cerebrum, gray matter, cortical gray matter, and caudate nucleus in males[3]. Clinical studies have further highlighted sex differences in FXS symptoms, with autistic behaviors, intellectual disability, and attention deficits more frequent in boys, while social interaction difficulties and mood disorders are more common in girls[4–6]. Recently, brain inflammation has gained more attention in the context of NDDs[7]. For example, immune system dysfunctions including altered plasma chemokine levels are reported in FXS[8–10]. Additionally, phenome-wide association studies suggest that FXS patients are at an increased risk of developing infectious diseases such as pneumonia, as well as autoimmune disorders like lupus erythematosus[11].

The responsible gene for FXS is *fragile X messenger ribonucleoprotein 1* (*FMR1*) on X chromosome, encoding an RNA-binding protein, fragile X messenger ribonucleoprotein (FMRP). FXS patients carry genetic variants of CGG trinucleotide repeat mutation in the *FMR1* gene, leading to loss-of-function of the protein[12]. FMRP is known to be widely expressed in the murine nervous system[13,14]. To model FXS and elucidate the role of FMRP, genetically engineered mice that lack the function of *Fmr1* gene (i.e., *Fmr1*-KO mice) have been developed[15]. *Fmr1*-KO mice exhibit abnormal synaptic plasticity and dendritic spine growth, which is linked to cognitive deficits[16,17].

Pioneering research on the role of FMRP and its target RNAs has primarily focused on mature neurons in the adult brain[18,19]. However, FMRP is also present in immature neurons and neural stem/progenitor cells, with its target mRNAs being studied during the mid-gestation[14,20,21]. A microarray study using fetal brain tissues from the hippocampus and cortex of *Fmr1*-KO mice (sex-unspecified) has revealed an overrepresentation of mGluR5-downstream signaling and immunological pathways[22]. Despite these insights, a comprehensive gene

[1]Department of Developmental Neuroscience, Tohoku University Graduate School of Medicine, Sendai, Miyagi, 980-8575, Japan. [2]Comparative Genomics Laboratory, National Institute of Genetics, Mishima, Shizuoka, 411-8540, Japan. [3]Department of Biochemistry and Cellular Biology, National Institute of Neuroscience, NCNP, Tokyo, 187-8502, Japan. ✉e-mail: takako.kikkawa.c4@tohoku.ac.jp; noriko.osumi.c7@tohoku.ac.jp

expression profile at the peak stage of neurogenesis, incorporating both male and female samples across all genotypes including a heterozygous (*Fmr1*-het) condition, has yet to be explored.

The current study aimed to obtain comprehensive transcriptomic datasets from the whole telencephalon samples of male wild-type (WT), male *Fmr1*-KO, female WT, female *Fmr1*-het, and female *Fmr1*-KO mice at embryonic day (E) 14.5, a peak stage of neurogenesis (Fig. 1a, n = 3 for each genotype). We conducted clustering analyses of bulk RNA-sequencing (RNA-seq) data, utilizing Principal Component Analysis (PCA) and hierarchical clustering to assess the similarities among biological groups. The clustering examinations found the groups differentiated by sex (male and female) and *Fmr1* dosages (WT, *Fmr1*-het, and *Fmr1*-KO) (Fig. 1b,c). Further examination of male and female sample groups showed that the majority of the transcripts were shared between the two sexes, while 4.8% were exclusive to males, and 7.0% to females (Fig. 1d). To visualize the overall data distribution of expression changes, the transcripts were plotted using minus-average (MA) plots (Fig. 2a–c), and *Fmr1* gene downregulation was confirmed in all *Fmr1*-deficient samples. Collectively, the data presented here provide a foundation for future studies aimed at enhancing the understanding of sex-specific phenotypes associated with *Fmr1* deficiency during this critical stage of embryonic brain development, facilitating a more accurate interpretation of functional studies.

Methods

Experimental animals. The animal experiments were carried out according to the National Institutes of Health guidelines outlined in the Guide for the Care and Use of Laboratory Animals. The Ethics Committee for Animal Experiment of Tohoku University Graduate School of Medicine approved all the experimental procedures described herein (2020-MDA-012-06). Male and female wild type (WT, C57BL/6 J) mice were purchased from CLEA Japan and used for maintaining the colony of *Fmr1*-knockout (KO) mice (originally B6.129P2-*Fmr1*^{tm1Cgr}/J, stock #003025, Jackson Laboratory) in the animal facility of Tohoku University Graduate School of Medicine and used in this study. Heterozygous (*Fmr1*-het) female mice were obtained either by crossing WT male mice with homozygous (*Fmr1*-KO) female mice, or by hemizygous (*Fmr1*-KO) male mice with WT female mice. For the RNA-sequencing samples, *Fmr1*-het female mice were crossed with either WT or *Fmr1*-KO male mice to obtain all five offspring genotypes (Fig. 1a; male WT, male *Fmr1*-KO, female WT, female *Fmr1*-het, and female *Fmr1*-KO). Embryonic day 0.5 (E0.5) was defined as midday on the day of vaginal plug detection.

DNA extraction and genotyping. Deoxyribonucleic acid (DNA) was extracted from the tail tissue of the samples. A mixture of 10 µl of 5x Colorless GoTaq® Flexi Buffer (Promega), 5 µl of 10% NP40 (Merck Millipore), 2 µl of Proteinase K (Sigma; 20 mg/ml) and 33 µl of milliQ water (mQ H_2O) was added to the mouse tissue and incubated overnight at 57 °C in a platform shaker. The sample was placed in a 90–95 °C water bath for 15 minutes, transferred on ice for 3 minutes, and centrifuged at 15,000 rpm for 5 minutes at 4 °C. The resulting extracted DNA was stored at 4 °C. Polymerase chain reaction (PCR) was performed using 1 µl of the extracted DNA and the GoTaq® Flexi DNA Polymerase (Promega) to determine sex using forward primer for *Ube1* 5′-TGGTCTGGACCCAAACGCTGTC-3′ and reverse primer for *Ube1* 5′-GGCAGCAGCCATCACATAATCC-3′[23]; as well as the WT and *Fmr1*-KO alleles of the samples using forward primer for *Fmr1* WT allele 5′-GTGGTTAGCTAAAGTGAGGATGATAAAGGGTG-3′, reverse primer for *Fmr1* WT allele 5′- CAGGTTTGTTGGGATTAACAGATCGTAGACG -3′, forward primer for *Fmr1*-KO allele 5′-CGCCTCAGAAGCCATAGAGCC-3′, and reverse primer for *Fmr1*-KO allele 5′-CATCGCCTTCTATCGCCTTCTTGAC-3′[15,21]. PCR was performed using the Vapo Protect Thermal Cycler (Eppendorf) as follows: For *Ube1*, 95 °C for 2 minutes, followed by 40 cycles of 95 °C for 15 seconds, 60 °C for 20 seconds, and 72 °C for 1 minute, with a final extension at 72 °C for 2 minutes. For *Fmr1*, 95 °C for 2 minutes, followed by 30 cycles of 95 °C for 30 seconds, 60 °C for 30 seconds, and 72 °C for 1 minute, with a final extension at 72 °C for 2 minutes. The amplified PCR products were visualized by electrophoresis on 3% or 1% agarose gels, respectively, using the Gel Doc™ EZ Imager (Bio-Rad).

Tissue collection. *Fmr1*-het female mice were used for mating with either WT or *Fmr1*-KO male mice to obtain five genotypes in offspring. The whole telencephalon of the resulting offspring at E14.5 was precisely dissected using fine forceps (REGINE #5) and micro-scissors (Leprex, LMB-50-7). The skin and skull tissues were carefully removed from the entire brain, and the whole telencephalon was dissected from the embryonic brain following previous methods[24,25]. The dissected tissue was immediately placed in the tubes filled with 200 µl of the RNAlater™ Stabilization Solution (Invitrogen) and stored at 4 °C for 24 h. Next, the solution was completely removed, and the tissue was snap frozen with liquid nitrogen and moved to −80 °C for long-term preservation. Tail samples were simultaneously collected from the embryos for sex determination and *Fmr1* genotyping using PCR.

RNA isolation. For RNA extraction, three samples were selected for each of the embryonic genotypes (male WT, male *Fmr1*-KO, female WT, female *Fmr1*-het, and female *Fmr1*-KO; n = 3 for each genotype). RNA was extracted from the telencephalon using the RNeasy Plus Mini Kit (QIAGEN). Prior to sequencing, the quality and quantity of RNA samples were analyzed using the TapeStation 4200 (Agilent). All samples submitted for sequencing displayed an acceptable RIN value ≥ 9.8 for RNA-seq analyses. RNA information together with sampling conditions are described in Supplementary Table S1.

Library preparation and RNA sequencing. Each library was prepared using 3 µg of total RNA with an Illumina Stranded mRNA Sample Prep Kit, following the manufacturer's protocol. Sequencing was performed on an Illumina NovaSeq 6000 with 100 bp paired-end reads (2 × 100 bp). RNA-seq data were processed using the Rhelixa RNA-seq pipeline (https://sc.ddbj.nig.ac.jp/en/advanced_guides/Rhelixa_RNAseq/Rhelixa_RNAseq) on the NIG supercomputer system. The pipeline included the following sequential steps:

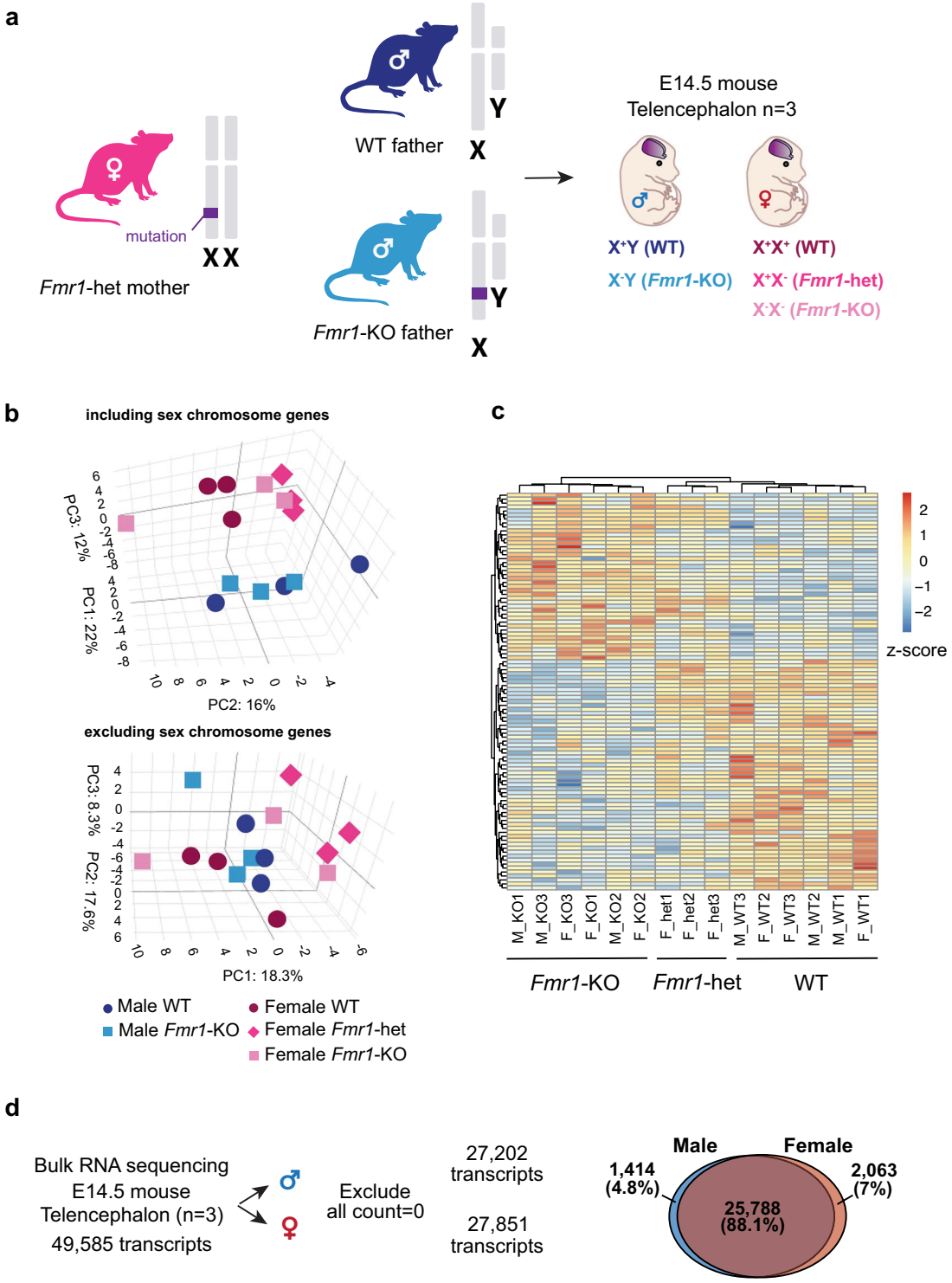

Fig. 1 Mating scheme to obtain samples for RNA sequencing experiment and the clustering analyses. (**a**) Mating strategy used to generate five possible offspring genotypes. *Fmr1*-het female mice were crossed with WT or *Fmr1*-KO male mice. Telencephalon tissues were collected at E14.5, including male WT (X^+Y), male *Fmr1*-KO (X^-Y), female WT (X^+X^+), female *Fmr1*-het (X^+X^-), and female *Fmr1*-KO (X^-X^-). (**b**) Three-dimensional PCA plots illustrating clustering of sample groups. The PCA plot in the upper graph represents all genes excluding genes with 0 variance, and the PCA plot in the lower graph represents an additional exclusion of sex chromosome genes from the analysis. PC1, PC2, and PC3 values are shown on the X-, Y-, and Z-axis, respectively. Sample groups are represented by distinct shapes and colors: male WT (dark blue circles), male *Fmr1*-KO (light blue squares), female WT (red circles), female *Fmr1*-het (dark pink diamonds), and female *Fmr1*-KO (light pink squares). (**c**) Hierarchical clustering and heatmap showing gene expression. The scale bar represents z-score normalization of the expression (count) values with the high expression levels indicated in red color and low expression levels in blue. The first six columns represent

Fmr1-KO (male and female *Fmr1*-KO), the next three columns represent female *Fmr1*-het, and the final six columns represent WT (male and female WT) samples. (**d**) Analysis of the number of sex specific transcripts. Whole telencephalon tissue from all biological groups (n = 3) was used for RNA extraction and sequencing, identifying 49,585 transcripts. These were divided into male (male WT and *Fmr1*-KO) and female (female WT, *Fmr1*-het, and *Fmr1*-KO) samples. After filtering out genes with zero raw counts in all groups, 27,202 transcripts remained in the male list and 27,851 in the female list. Of these, 88.1% of the genes were shared, with 4.8% unique to males and 7% unique to females.

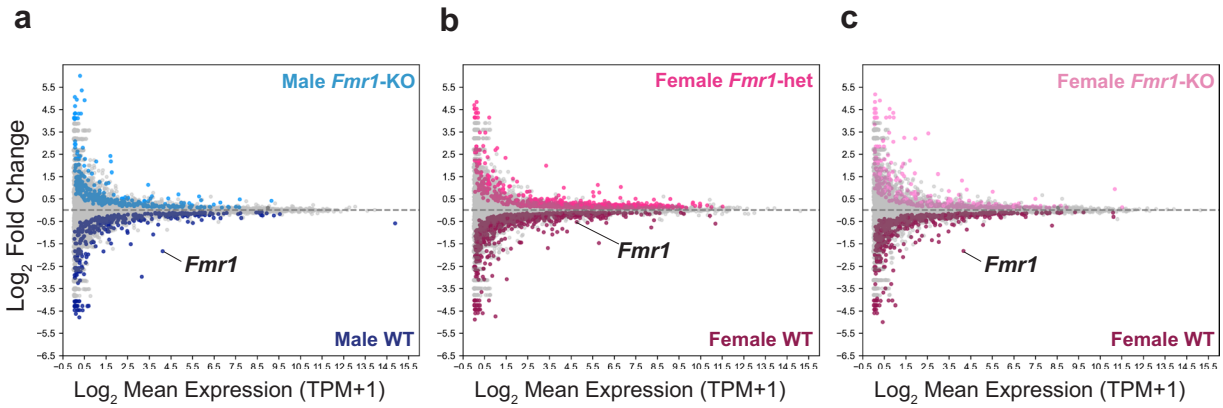

Fig. 2 Data distribution and differential expression of *Fmr1* gene in E14.5 telencephalon of *Fmr1*-mutant mouse embryos. MA plots illustrating overall data distribution by comparing male WT vs *Fmr1*-KO, female WT vs *Fmr1*-het, and female WT vs *Fmr1*-KO. Transcripts with significant differential expression ($p < 0.05$) are highlighted using colored datapoints, and *Fmr1* gene symbol is indicated for each comparison. The Y-axis represents $\log_2$ fold change, while the X-axis indicates the $\log_2$ of the mean of normalized gene expression levels (TPM + 1) between groups (see Methods for more details). (**a**) Comparison of male WT (dark blue) vs male *Fmr1*-KO (light blue). (**b**) Comparison of female WT (red) vs female *Fmr1*-het (pink). (**c**) Comparison of female WT (red) vs female *Fmr1*-KO (light pink).

(1) Quality assessment using FastQC v0.11.7 (--nogroup) (https://www.bioinformatics.babraham.ac.uk/projects/fastqc/)
(2) Adapter removal and quality trimming using Trimmomatic v0.38[26] (ILLUMINACLIP:paired_end.fa:2:30:10, LEADING:20, TRAILING:20, SLIDINGWINDOW:4:15, MINLEN:36) with both Illumina standard and custom adapter sequences
(3) Strand information assessment using RSeQC v3.0.1[27] (infer_experiment.py) with the mm10 RefSeq Gene annotation
(4) Read mapping to the mm10 reference genome using HISAT2 v2.1.0[28] (--rna-strandness RF, --dta)
(5) BAM file conversion and sorting using SAMtools v1.9[29] (view, sort, index)
(6) Read counting using featureCounts v1.6.3[30] (-p, -s 2, -T 4, -F GTF, -t exon, -g gene_id) against the Ensembl annotation (Mus_musculus.GRCm38.87).

Library complexity was estimated using Picard v3.1.1 (EstimateLibraryComplexity) with default parameters (http://broadinstitute.github.io/picard/). Coverage metrics for exonic regions were calculated using bedtools v2.29.1[31] (coverage) based on the same Ensembl annotation. ERCC spike-in normalization was not applied. Library details, including sample information, are provided in Supplementary Table S1.

Principal Component Analysis (PCA) and hierarchical clustering. Inter-group comparisons were conducted among all samples after that gene expression levels were normalized using the variance stabilizing transformation (VST) function from the DESeq2 package version 1.36.0 in R. Principal Component Analysis (PCA) was performed with the prcomp function in R on all genes excluding the genes displaying 0 variance values, as well as a second analysis which excluded the sex chromosome genes. A three-dimensional scatter plot was visualized with the plot_ly package version 4.10.3, using PC1, PC2, and PC3 values as the X-, Y-, and Z-axis, respectively. Additionally, a heatmap with hierarchical clustering was generated using the pheatmap package version 1.0.12 in R from the top 100 genes based on the *p*-value estimated by count values of WT and *Fmr1*-mutant mice, and z-score normalization was applied to the gene expression data.

Selection of genes applied for sex-specific transcript number analysis. A total of 49,585 transcripts in this dataset were divided into male (male WT and *Fmr1*-KO) and female (female WT, *Fmr1*-het, and *Fmr1*-KO) groups. Genes with zero raw counts across all samples in each group were filtered out, resulting in 27,202 transcripts in males and 27,851 in females. A substantial overlap was observed, with 88.1% of the genes being shared between the two lists, while 4.8% were found exclusively in males, and 7% were unique to females (Fig. 1d).

Venn diagram. The Venn diagram (Fig. 1d) was generated using R (version 4.4.2), which shows the number of transcripts with non-zero counts in male and female sample groups, illustrating the overlap and sex-specific expression of genes.

Statistical analysis. Data from all transcripts were analyzed to assess statistical significance among sample groups, calculated by the Bioconductor package edgeR[32–34] in R using raw count values. For each comparison, edgeR conducted an exact test followed by the Benjamini-Hochberg test and reported *p*-values for individual transcripts. To control the false discovery rate (FDR), *p*-values were adjusted using the Benjamini-Hochberg procedure implemented in edgeR. *Fmr1* gene downregulation was confirmed by observing significant FDR values in the *Fmr1*-deficint samples (FDR < 0.1), comparing male WT vs male *Fmr1*-KO, female WT vs female *Fmr1*-het, and female WT vs female *Fmr1*-KO (Fig. 2a–c). Additionally, sex-specific expression of the sex chromosome related genes was confirmed similarly in male and female samples, comparing male WT vs female WT and male *Fmr1*-KO vs female *Fmr1*-KO (FDR < 0.1).

MA plots. The MA plots (Fig. 2a–c) were generated using Python with the bioinfokit toolkit (version 2.1.4)[35]. These plots display the $\log_2$ fold change (Log2FC) in gene expression between each condition (calculated by edgeR[32–34]) on the vertical axis. The horizontal axis represents the $\log_2$ of the mean of normalized gene expression levels (TPM + 1) of two conditions, where "TPM + 1" values were used to avoid invalid numerical outcomes. Comparisons were made for male WT vs male *Fmr1*-KO, female WT vs female *Fmr1*-het, and female WT vs female *Fmr1*-KO. Transcripts with differential expression in each condition ($p < 0.05$) are highlighted with colored datapoints in the MA plots, and *Fmr1* gene datapoint is indicated in each graph.

Data Records

The 15 files of raw RNA-seq data derived from all the five biological groups (three replicates of male WT, male *Fmr1*-KO, female WT, female *Fmr1*-het, and female *Fmr1*-KO) have been deposited in the DNA Data Bank of Japan (DDBJ) (BioProject accession number: PRJDB18779)[36]. The DDBJ BioSample accession numbers of each sample are shown in Supplementary Table S1.

The expression values (counts) were deposited in the DDBJ Genomic Expression Archive (GEA) (GEA accession number: E-GEAD-870)[37], and the relevant fastq file names of each sample are shown in Supplementary Table S1.

The following file related to the TPM and count values of all the transcripts presented in the RNA-seq data have been deposited in figshare[38]:

All_Transcripts_Expression_TPM_Count.xlsx

Technical Validation

Sample information. For the bulk RNA-seq analysis, three embryos for each of the five biological groups (male WT, male *Fmr1*-KO, female WT, female *Fmr1*-het, and female *Fmr1*-KO) at E14.5 were used. Each replicate of the three male WT and three male *Fmr1*-KO samples were selected from three different litters. The three female WT samples originated from the same litters as the male WT samples, all with WT fathers. Each replicate of the three female *Fmr1*-het and three female *Fmr1*-KO samples were selected from three different litters, one of which is used for the male samples (Supplementary Table S1). To ensure consistency, all the embryos were selected based on similar body size, an indicator of comparable developmental stages.

RNA quality check. The quality and quantity of RNA samples used for this study were assessed using the TapeStation 4200 (Agilent). We evaluated total RNA concentration, total amount, 260/280 and 260/230 ratios, as well as RNA Integrity Number (RIN). All samples submitted for sequencing had RIN value ≥ 9.8, which is sufficient for RNA-seq analyses (Supplementary Table S1).

RNA-seq clustering by sex and *Fmr1* gene dosage. To validate the data collection procedure, inter-group comparisons were performed among WT, *Fmr1*-het, and *Fmr1*-KO samples from the RNA-seq experiment using Principal Component Analysis (PCA) and hierarchical clustering (Fig. 1b,c). In the initial PCA, the combined contribution of PC1 and PC2 accounted for less than 40% of the total variance, making it difficult to fully capture clustering trends in two dimensions. Therefore, a 3D visualization approach was employed to better illustrate sex-biased clustering patterns (Fig. 1b).

The PCA revealed clear separation of samples into male and female clusters (Fig. 1b, upper panel), with PC1, PC2, and PC3 explaining 22%, 16.0%, and 12.0% of the variance, respectively, consistent with our previous transcriptomic analysis of mouse embryonic brains at E14.5[25]. This finding aligns with prior observations that sex differences in the mouse telencephalic transcriptome emerge as early as mid-gestation, before the perinatal surge of testosterone. To further asses the contribution of sex chromosome-linked transcripts, sex chromosome genes were excluded (Fig. 1b, lower panel), in which PC1, PC2, and PC3 accounted for 18.3%, 17.6%, and 8.3% of variance, respectively. The results indicated that sex chromosome gene expression plays a major role in the separation of male and female samples. In its absence, male and female clusters were less distinct. Additionally, both PCA plots revealed that the WT and mutant females were relatively far apart (except for one *Fmr1*-KO sample), whereas WT and mutant males showed minimal separation (Fig. 1b). Furthermore, hierarchical clustering based on the top 100 DEGs ($p < 0.05$) demonstrated distinct expression patterns among biological groups, with clear separation according to *Fmr1* gene dosage (WT, *Fmr1*-het, and *Fmr1*-KO; Fig. 1c).

Differential transcription by *Fmr1* gene dosage and sex. To visualize overall expression changes across conditions, MA plots were generated, displaying $\log_2$ fold change (Log2FC) between groups on the vertical axis and $\log_2$ of the mean of normalized gene expression levels (TPM + 1) between groups on the horizontal axis

(see "MA plots" in the Methods section for further details). Three comparisons were performed: male WT vs male *Fmr1*-KO, female WT vs female *Fmr1*-het, and female WT vs female *Fmr1*-KO, and the transcripts with differential expression in each condition ($p < 0.05$) were highlighted with colored datapoints (Fig. 2a–c).

The *Fmr1* gene was significantly downregulated in both *Fmr1*-het (FDR < 0.001) and *Fmr1*-KO conditions (FDR = 1.67E-79 in male; FDR = 6.87E-78 in female), confirming the expected genotype across all samples (Fig. 2a–c).

Additionally, comparison of male and female samples under both WT and *Fmr1*-mutant conditions revealed a significantly differential expression of sex chromosome-related genes including *Xist*, *Kdm5c*, *Kdm6a*, and *Eif2s3x* on the X chromosome, and *Ddx3y*, *Uty*, *Kdm5d*, and *Eif2s3y* on the Y chromosome (FDR < 0.1). These DEGs identified in comparison of sexes is consistent with previous literature[25,39–41] supporting the validity of our data, and confirming the sex assessment for all the samples.

Usage Notes

It is important to note that there is individual variability in the expression data across our samples, as observed in the hierarchical clustering heatmap (Fig. 1c) and the individual TPM values in the figshare database[38] which also show subtle transcriptional changes. This variability may be attributed to the small sample size (n = 3) in the RNA-seq experiment. We acknowledge the size limitation of our dataset and strongly recommend prioritizing higher gene expression data (such as TPM > 20) for further analysis.

Our data focuses on a single developmental time point, which limits the temporal scope of the dataset. Consequently, it does not provide insights into how *Fmr1* deficiency alters the pace of sexual differentiation or how these phenotypes evolve over time during brain development. Further studies providing insight into early and late developmental stages are necessary to fully understand the persistence and implications of these transcriptional alterations in *Fmr1* deficiency throughout brain development.

Code availability

The open access software and versions mentioned in the main text were utilized for quality control and data analysis as described in the methods.

1. The University of California Santa Cruz (UCSC) Genome Browser was used to annotate mouse genetic information[42,43]: http://hgdownload.soe.ucsc.edu/goldenPath/mm10/database/
2. R software (v4.2.2) and The Bioconductor packages DESeq2 version 1.36.0 and edgeR version 3.16 were applied for performing clustering analysis and obtaining statistical differences and fold changes among RNA-seq groups, respectively[32–34]: https://bioconductor.org/packages/release/bioc/html/DESeq2.html http://bioconductor.jp/packages/release/bioc/html/edgeR.html
3. The following R packages were utilized: 'prcomp' for applying the PCA in Fig. 1b, 'plot_ly' version 4.10.3 to generate the 3D PCA plot in Fig. 1b, 'pheatmap' version 1.0.12 for generating the hierarchical clustering heatmap in Fig. 1c, and 'VennDiagram' for Fig. 1d.
4. The Python toolkit 'bioinfokit'[35] version 2.1.4 was used for generating the MA plots in Fig. 2a–c: https://github.com/reneshbedre/bioinfokit

All codes and scripts used for data analysis in this study can be found in the following links and articles: http://hgdownload.soe.ucsc.edu/goldenPath/mm10/database/, https://seaborn.pydata.org/, https://www.r-project.org/help.html.

Received: 4 November 2024; Accepted: 28 April 2025;
Published online: 02 June 2025

References

1. Ciaccio, C. *et al*. Fragile X syndrome: a review of clinical and molecular diagnoses. *Ital J Pediatr* **43**, 39 (2017).
2. Hunter, J. *et al*. Epidemiology of fragile X syndrome: A systematic review and meta-analysis. *Am J Med Genet A* **164**, 1648–1658 (2014).
3. Eliez, S. Brain anatomy, gender and IQ in children and adolescents with fragile X syndrome. *Brain* **124**, 1610–1618 (2001).
4. Reiss, A. L., Freund, L., Vinogradov, S., Hagerman, R. & Cronister, A. Parental inheritance and psychological disability in fragile X females. *Am J Hum Genet* **45**, 697–705 (1989).
5. Freund, L. S. Chromosome Fragility and Psychopathology in Obligate Female Carriers of the Fragile X Chromosome. *Arch Gen Psychiatry* **49**, 54 (1992).
6. Baker, E. K. *et al*. Intellectual functioning and behavioural features associated with mosaicism in fragile X syndrome. *J Neurodev Disord* **11**, 41 (2019).
7. Deverman, B. E. & Patterson, P. H. Cytokines and CNS Development. *Neuron* **64**, 61–78 (2009).
8. Ashwood, P., Nguyen, D. V., Hessl, D., Hagerman, R. J. & Tassone, F. Plasma cytokine profiles in Fragile X subjects: Is there a role for cytokines in the pathogenesis? *Brain Behav Immun* **24**, 898–902 (2010).
9. Careaga, M. *et al*. Group I metabotropic glutamate receptor mediated dynamic immune dysfunction in children with fragile X syndrome. *J Neuroinflammation* **11**, 110 (2014).
10. Van Dijck, A. *et al*. Reduced serum levels of pro-inflammatory chemokines in fragile X syndrome. *BMC Neurol* **20**, 138 (2020).
11. Yu, K. -H. *et al*. The phenotypical implications of immune dysregulation in fragile X syndrome. *Eur J Neurol* **27**, 590–593 (2020).
12. Verkerk, A. J. M. H. *et al*. Identification of a gene (*FMR-1*) containing a CGG repeat coincident with a breakpoint cluster region exhibiting length variation in fragile X syndrome. *Cell* **65**, 905–914 (1991).
13. Darnell, J. C. *et al*. FMRP Stalls Ribosomal Translocation on mRNAs Linked to Synaptic Function and Autism. *Cell* **146**, 247–261 (2011).
14. Saffary, R. & Xie, Z. FMRP Regulates the Transition from Radial Glial Cells to Intermediate Progenitor Cells during Neocortical Development. *The Journal of Neuroscience* **31**, 1427–1439 (2011).
15. *Fmr1* knockout mice: a model to study fragile X mental retardation. The Dutch-Belgian Fragile X Consortium. *Cell* **78**, 23–33 (1994).

16. Huber, K. M., Gallagher, S. M., Warren, S. T. & Bear, M. F. Altered synaptic plasticity in a mouse model of fragile X mental retardation. *Proceedings of the National Academy of Sciences* **99**, 7746–7750 (2002).
17. Comery, T. A. *et al*. Abnormal dendritic spines in fragile X knockout mice: Maturation and pruning deficits. *Proceedings of the National Academy of Sciences* **94**, 5401–5404 (1997).
18. Brown, V. *et al*. Microarray Identification of FMRP-Associated Brain mRNAs and Altered mRNA Translational Profiles in Fragile X Syndrome. *Cell* **107**, 477–487 (2001).
19. Maurin, T. *et al*. HITS-CLIP in various brain areas reveals new targets and new modalities of RNA binding by fragile X mental retardation protein. *Nucleic Acids Res* **46**, 6344–6355 (2018).
20. Pilaz, L.-J., Lennox, A. L., Rouanet, J. P. & Silver, D. L. Dynamic mRNA Transport and Local Translation in Radial Glial Progenitors of the Developing Brain. *Current Biology* **26**, 3383–3392 (2016).
21. Casingal, C. R., Kikkawa, T., Inada, H., Sasaki, Y. & Osumi, N. Identification of FMRP target mRNAs in the developmental brain: FMRP might coordinate Ras/MAPK, Wnt/β-catenin, and mTOR signaling during corticogenesis. *Mol Brain* **13**, 167 (2020).
22. Prilutsky, D. *et al*. Gene expression analysis in *Fmr1*KO mice identifies an immunological signature in brain tissue and mGluR5-related signaling in primary neuronal cultures. *Mol Autism* **6**, 66 (2015).
23. Chuma, S. & Nakatsuji, N. Autonomous Transition into Meiosis of Mouse Fetal Germ Cells *in Vitro* and Its Inhibition by gp130-Mediated Signaling. *Dev Biol* **229**, 468–479 (2001).
24. Rehen, S. K. *et al*. A new method of embryonic culture for assessing global changes in brain organization. *J Neurosci Methods* **158**, 100–108 (2006).
25. Ochi, S. *et al*. A Transcriptomic Dataset of Embryonic Murine Telencephalon. *Sci Data* **11**, 586 (2024).
26. Bolger, A. M., Lohse, M. & Usadel, B. Trimmomatic: a flexible trimmer for Illumina sequence data. *Bioinformatics* **30**, 2114–2120 (2014).
27. Wang, L., Wang, S. & Li, W. RSeQC: quality control of RNA-seq experiments. *Bioinformatics* **28**, 2184–2185 (2012).
28. Kim, D., Paggi, J. M., Park, C., Bennett, C. & Salzberg, S. L. Graph-based genome alignment and genotyping with HISAT2 and HISAT-genotype. *Nat Biotechnol* **37**, 907–915 (2019).
29. Danecek, P. *et al*. Twelve years of SAMtools and BCFtools. *Gigascience* **10** (2021).
30. Liao, Y., Smyth, G. K. & Shi, W. featureCounts: an efficient general purpose program for assigning sequence reads to genomic features. *Bioinformatics* **30**, 923–930 (2014).
31. Quinlan, A. R. & Hall, I. M. BEDTools: a flexible suite of utilities for comparing genomic features. *Bioinformatics* **26**, 841–842 (2010).
32. Robinson, M. D., McCarthy, D. J. & Smyth, G. K. edgeR: a Bioconductor package for differential expression analysis of digital gene expression data. *Bioinformatics* **26**, 139–140 (2010).
33. McCarthy, D. J., Chen, Y. & Smyth, G. K. Differential expression analysis of multifactor RNA-Seq experiments with respect to biological variation. *Nucleic Acids Res* **40**, 4288–4297 (2012).
34. Chen, Y., Lun, A. T. L. & Smyth, G. K. From reads to genes to pathways: differential expression analysis of RNA-Seq experiments using Rsubread and the edgeR quasi-likelihood pipeline. *F1000Res* **5**, 1438 (2016).
35. Bedre R. Bioinformatics data analysis and visualization toolkit. https://github.com/reneshbedre/bioinfokit (2020).
36. Ebrahimiazar, S. *et al*. Raw data files at DNA Data Bank of Japan. https://ddbj.nig.ac.jp/resource/bioproject/PRJDB18779 (2025).
37. Ebrahimiazar, S. *et al*. Expression data files at the Genomic Expression Archive. https://ddbj.nig.ac.jp/public/ddbj_database/gea/experiment/E-GEAD-000/E-GEAD-870/ (2025).
38. Ebrahimiazar, S. *et al*. Figshare database file. https://doi.org/10.6084/m9.figshare.27177891 (2025).
39. Dewing, P., Shi, T., Horvath, S. & Vilain, E. Sexually dimorphic gene expression in mouse brain precedes gonadal differentiation. *Molecular Brain Research* **118**, 82–90 (2003).
40. Szakats, S., McAtamney, A., Cross, H. & Wilson, M. J. Sex-biased gene and microRNA expression in the developing mouse brain is associated with neurodevelopmental functions and neurological phenotypes. *Biol Sex Differ* **14**, 57 (2023).
41. Paylar, B., Pramanik, S., Bezabhe, Y. H. & Olsson, P.-E. Temporal sex specific brain gene expression pattern during early rat embryonic development. *Front Cell Dev Biol* **12**, (2024).
42. Karolchik, D. The UCSC Genome Browser Database. *Nucleic Acids Res* **31**, 51–54 (2003).
43. Nassar, L. R. *et al*. The UCSC Genome Browser database: 2023 update. *Nucleic Acids Res* **51**, D1188–D1195 (2023).

Acknowledgements

We would like to thank Dr. Shinpei Kawaoka for valuable comments. We are grateful to Ms. Sayaka Makino for assistance in maintaining experimental animals. S. Ebrahimiazar was supported by Neuro Global Program, Tohoku University. This research was funded by AMED (#JP21wm0425003), JSPS KAKENHI funding (#19H03318, 24K02203) to N.O. This work was also supported by JSPS KAKENHI funding (#16H06279 (PAGS)), AMED (#JP24wm0625311), The Mochida Memorial Foundation for Medical and Pharmaceutical Research (Japan), Takeda Science Foundation (Japan), The Program for Creation of Interdisciplinary Research in Frontier Research Institute for Interdisciplinary Sciences in Tohoku University to T.K. A part of this study was supported by the Support System for Young Researchers to use research equipment, instruments, and devices at Tohoku University.

Author contributions

Conceptualization, S.E., T.K. and N.O.; preparation for RNA-seq, T.K., Y.M. and A.T.; data process, S.E. T.K., Y.M., Sa.M., Sh.M., M.H. and A.T.; data deposition, T.K., Y.M. and A.T.; figure preparation, S.E. and Sa.M.; writing review and editing, S.E., T.K. and N.O.; supervision, N.O.; project administration, S.E., T. K. and N.O.; funding acquisition, T.K. and N.O. All authors have read and agreed to the published version of the manuscript.

Competing interests

The authors declare no competing interests.

Additional information

Supplementary information The online version contains supplementary material available at https://doi.org/10.1038/s41597-025-05104-7.

Correspondence and requests for materials should be addressed to T.K. or N.O.